# Seismic wavepropagation concepts applied to the interpretation of marine controlled-source electromagnetics

*Rune Mittet*, EMGS*




## SUMMARY

Concepts like reflections, refractions, diffractions and transmissions are very useful for the interpretation of seismic data. Moreover, these concepts play a key role in the design of processing algorithms for seismic data. Currently, however, the same concepts are not widely used for the analysis and interpretation of marine controlled-source electromagnetic (marine CSEM) data. Connections between seismic and marine CSEM data are established by analytically transforming the diffusive Maxwell equations to wave-domain Maxwell equations. Both seismic data and wave-domain electromagnetic data are simulated with 3D finite-difference schemes. The two data types are similar, however, the wave-domain electromagnetic data must be transformed back to the diffusive domain to properly describe realistic field propagation in the earth. The inverse transform from the wave domain to the diffusive domain is analyzed. Concepts like reflections, refractions, diffractions and transmissions are valid also for marine CSEM data but the properties of the inverse transform favor refracted and guided events over reflected and diffracted events. In this sense, marine CSEM data are similar to refraction seismic data.


## INTRODUCTION

Concepts like reflections, refractions, diffractions and transmissions are very useful for the interpretation of seismic data. Likewise, these concepts also play a key role in the design of processing algorithms for seismic data. Currently, however, the same concepts are not widely used for the analysis and interpretation of marine controlled-source electromagnetic (marine CSEM) data. Here I will demonstrate that these seismic wavepropagation concepts can be applied to the interpretation of marine CSEM data. By establishing connections between seismic and marine CSEM data I hope to make marine CSEM data more accessible to those who today have a basic understanding of seismic wavepropagation.

Low frequency electromagnetic fields as we observe them in marine CSEM surveys are diffusive in nature. For the frequency domain Maxwell equations we know that the ratio of the imaginary part of the wavenumber to the real part of the wavenumber is of order unity. Lossless and dispersionless field propagation will happen if the imaginary part of the wavenumber is zero and if the phase velocity is independent of frequency. Although this is an approximation that is often used for seismic wave propagation, it is not realistic. Absorption and dispersion effects are present in observed seismic wavefields. Thus, a description of realistic seismic wave propagation requires both a complex wavenumber to account for absorption effects and a frequency-dependent phase velocity to give proper causal fields. The frequency dependence of the phase velocity is a consequence of the Kramers-Kronig relation for the real and imaginary part of the wavenumber. Absorption of seismic data is commonly quantified by the dimensionless quality factor, $Q$. If the absorption effects are not too extreme we find that the ratio of the imaginary part of the wavenumber to the real part of the wavenumber is approximately $\frac{1}{2Q}$. The Q factor for sedimentary rocks can be as low as 10, but more common values are $Q \sim 30 - 200$ . Thus the ratio of the imaginary part of the wavenumber to the real part of the wavenumber is typically one to two orders of magnitude smaller for seismic wave propagation when we compare with low frequency electromagnetic field propagation. A seismic wave with $Q$ of order 1 will behave in the same manner as a low frequency electromagnetic field typical for marine CSEM.

Concepts like reflections and transmissions are used in the analysis of anelastic seismic wavepropagation. The reflection and transmission coefficients are fully determined by the relevant boundary conditions. Carcione (2007) discusses a correspondence principle for seismic waves where a viscoelastic solution can be obtained if the elastic solution is known. The procedure involves replacing the elastic moduli with the corresponding viscoelastic moduli. This correspondence principle can be applied to the analysis of reflection and transmission coefficients. There is no limitation on the absorption strength when it comes to the validity of this approach. We do not have to abandon classical concepts like reflections and transmissions even for very strong absorption. There are no reasons to abandon these concepts for low-frequency electromagnetic fields. Reflection and transmission coefficients are the result of analyzing boundary conditions for incoming plane waves at plane boundaries. These boundary conditions must be operative for both loss-less and lossy fields. However, the frequency dependent behavior of wavenumbers, reflection coefficients and transmission coefficients can give rise to very different field behavior depending on whether the absorption effects are weak or strong.

The analysis provided here is based on a transform method for solving parabolic partial differential equations. The key element of the transform method is that a parabolic partial differential equation can be analytically transformed to a corresponding second-order hyperbolic partial differential equation. The solution of the hyperbolic partial differential equation can then subsequently be back-transformed to give the solution to the proper parabolic partial differential equation. This inverse transform is over the time axis only. Parabolic partial differential equation are typical for diffusion problems whereas second-order hyperbolic partial differential equation are typical for wave propagation problems. A partial differential equation of the first order in the time derivatives and second order in the spatial derivatives will be parabolic whereas a partial differential equation of the second order in the time derivatives and second order in the spatial derivatives will be second-order hyperbolic. A very elegant and useful analysis of this transformation method is given by de Hoop (1996). His formulation

of the correspondence principle for time-domain electromagnetic wave and diffusion fields is essential to the discussion that follows.

The present paper demonstrates similarities between seismic wave propagation and field propagation relevant for marine CSEM. The seismic wave fields will be approximated by acoustic fields in this work. The acoustic approximation is sufficient to demonstrate the points I want to make here. The fields in both the acoustic and electromagnetic examples will be calculated by 3D finite differences. The electromagnetic example may potentially cause some misunderstanding. The electromagnetic field prior to the transform to the frequency domain is in a fictitious time domain. This field behaves like a lossless wave. The transform function that takes the field back to the diffusive, "real world", is known and fairly simple. A key element is to understand the effect of the transform from the fictitious domain to the diffusive domain. It will be clear from the examples that the electromagnetic fields in the fictitious domain share properties like reflection, transmission, refraction and diffraction with the acoustic fields. The question to answer is which of these modes survive the inverse transform from the fictitious time domain to the diffusive frequency domain.

## THEORY

We shall here be concerned with both acoustic and electromagnetic field propagation. The underlying simulation method will in both cases be 3D high-order finite differences. The electromagnetic fields will be analyzed in both the time and the frequency domain.

### The seismic case

The acoustic wave propagation problem is given by Newton's second law and the constitutive relations,

$$\begin{aligned} \nabla\cdot\mathbf{v}(\mathbf{x},t)+\kappa(\mathbf{x})\partial_t P(\mathbf{x},t) &= 0, \\ \nabla P(\mathbf{x},t)+\rho_{ac}(\mathbf{x})\partial_t\mathbf{v}(\mathbf{x},t) &= \mathbf{f}(\mathbf{x},t), \end{aligned} \tag{1}$$

where $\mathbf{v}$ is particle velocity, $P$ is pressure, $\mathbf{f}$ is a force-density source function, $\kappa$ is the compliance and $\rho_{ac}$ is the density. For the simulations performed here the density will be kept constant at 1000 kg/m$^3$. The propagation velocity is given by the compliance and density as,

$$c(\mathbf{x})=\sqrt{\frac{1}{\rho_{ac}\kappa(\mathbf{x})}}. \tag{2}$$

### The electromagnetic case

The electromagnetic part of the present work is based on Mittet (2010) which again is based on Lee et al. (1989) and de Hoop (1996). In particular, Mittet (2010) follows the formulation of de Hoop (1996), the main difference is that Mittet (2010) uses Fourier transforms from time to frequency whereas de Hoop (1996) uses Laplace transforms.

The Maxwell equations in the quasi-static limit are,

$$\begin{aligned} -\nabla\times\mathbf{H}(\mathbf{x},t)+\sigma(\mathbf{x})\mathbf{E}(\mathbf{x},t) &= -\mathbf{J}(\mathbf{x},t), \\ \nabla\times\mathbf{E}(\mathbf{x},t)+\mu\partial_t\mathbf{H}(\mathbf{x},t) &= 0, \end{aligned} \tag{3}$$

where $\mathbf{E}$ and $\mathbf{H}$ are electric and magnetic vector fields. The source term is the electric current density, $\mathbf{J}$. The conductivity is $\sigma$. The magnetic permeability $\mu$ is assumed isotropic and equal to the value in vacuum. This is a common assumption for sedimentary rocks. The electromagnetic field in the simulation examples is excited with an electric current density in the $x$-direction.

The isotropic non-diffusive representation of the Maxwell equations is,

$$\begin{aligned} -\nabla\times\mathbf{H}'(\mathbf{x},t')+\varepsilon'(\mathbf{x})\partial_{t'}\mathbf{E}'(\mathbf{x},t') &= -\mathbf{J}'(\mathbf{x},t'), \\ \nabla\times\mathbf{E}'(\mathbf{x},t')+\mu\partial_{t'}\mathbf{H}'(\mathbf{x},t') &= 0, \end{aligned} \tag{4}$$

where $\varepsilon'(\mathbf{x})$ is the electric permittivity. The primes for the electric fields, the magnetic fields and the electric permittivity in equation 4 are used to distinguish these fields from the diffusive fields in equation 3. The reason for this is that there is a transformation relation between the non-diffusive field in equation 4 and the diffusive field in equation 3 if,

$$\sigma(\mathbf{x})=2\omega_0\varepsilon'(\mathbf{x}), \tag{5}$$

where $\omega_0$ is an arbitrary positive constant. The primed fields must be viewed as existing in a fictitious time domain. The transformation relation is discussed in detail in Mittet (2010) where it is demonstrated that solving the problem in equation 4 with equation 5 gives sufficient information to obtain the field solutions to the diffusive problem in equation 3.

The propagation velocity in equation 4 is given by the magnetic permeability and electric permittivity as,

$$c(\mathbf{x})=\sqrt{\frac{1}{\mu\varepsilon'(\mathbf{x})}}. \tag{6}$$

Note that the propagation velocity in equation 6 can be written

$$c(\mathbf{x})=\sqrt{\frac{2\omega_0\rho(\mathbf{x})}{\mu}}, \tag{7}$$

with the resistivity $\rho(\mathbf{x})$ as the reciprocal of conductivity.

From the fictitious time domain to the real frequency domain the transformation relation between the electric field components is,

$$E_i(\mathbf{x},\omega)=\int_0^T dt' {E'}_i(\mathbf{x},t')e^{-\sqrt{\omega\omega_0}t'}e^{i\sqrt{\omega\omega_0}t'}. \tag{8}$$

This is equation 17 in Mittet (2010) and is also the equation I will use here when I analyze the electromagnetic field propagation. The transform in equation 8 is valid with the constraint that ${E'}_i(\mathbf{x},t')$ is causal, hence we must ensure ${E'}_i(\mathbf{x},t'\le 0)=0$.

## RESULTS

Before we can proceed to the simulation examples, I need to comment on the use of terms like reflection, transmission, refraction, diffraction and guided field as used here: Some of

these terms have different meanings within different fields of physics. The terminology used here is the one most commonly used in the analysis of seismic data.

### The seismic case

I will first present results from a seismic/acoustic simulation. It is a deep water case with generally high propagation velocities in the formation. The results from the simulation of seismic data in this model will be compared to electromagnetic data simulated in an analogous model. A cross section of the velocity model used for the acoustic example is shown in Figure 1. The model is invariant normal to this cross section.

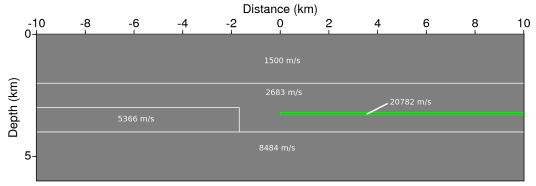


Figure 1: The cross section of the 3D velocity model.

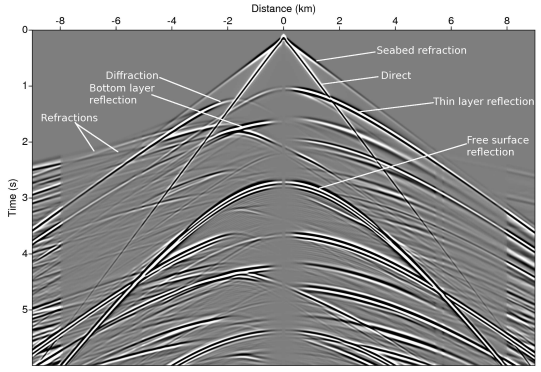


Figure 2: Normalized shotgather for the vertical component of particle velocity.

The source is placed at distance $x_s = 0$ km and $y_s = 0$ km. The source depth is $z_s = 1.96$ km. Receivers are placed on the seabed from distance - 9 km to distance 9 km in $x$ and at $y = 0$ km. The time behavior of the vertical force density used equals a first-order derivative of a Gaussian with a maximum frequency of 23 Hz. The grid steplengths are 20 m in all three spatial directions.

Figure 2 is a normalized shotgather for the acoustic simulation. The recorded data is the vertical component of particle velocity. Some of the events are tagged. This will simplify the comparison with the electromagnetic simulation discussed below. Note that the seabed refracted event is the first arrival even at very small offsets and that the moveout is linear.

### The electromagnetic case

We next proceed to the electromagnetic case. A cross section of the resistivity model used for the marine CSEM example is shown in Figure 3. This model has the same geometry as the velocity model in Figure 1. The waterlayer has a resistivity of 0.3125 ohm-m, the top formation has a resistivity of 1.0 ohm-m, the 1 km thick layer on the left side of the model has a resistivity of 4 ohm-m and the bottom layer has a resistivity of 10.0 ohm-m. These are all realistic formation resistivities. The thin layer on the right hand side of the model has a resistivity of 60.0 ohm-m which is a realistic value for a hydrocarbon filled reservoir. Note that the resistivity model in Figure 3 is mapped to the velocity model given in Figure 1 by the resistivity-velocity transformation given in equation 7 if $\omega_0 = 2\pi f_0$ with $f_0 = 0.7198$ Hz.

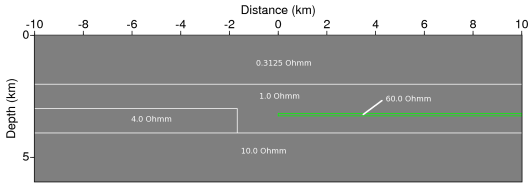


Figure 3: The cross section of the 3D resistivity model.

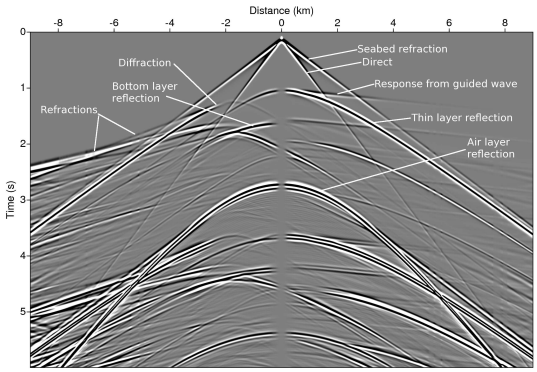


Figure 4: Normalized shotgather for the inline electric field.

The temporal behavior of the transmitter current is identical to the temporal behavior of the vertical force density used as source for the acoustic simulation. Source and receiver locations are identical to those for the acoustic simulations. The grid steplengths are 20 m in all three spatial directions.

Figure 4 is a normalized shotgather for the electromagnetic simulation. This shotgather shows mostly the same events as the acoustic shotgather in Figure 2. The main difference is the response from a guided wave which is present in the electromagnetic data but not in the acoustic data. The cause of the guided wave is the thin resistive layer marked in green in Figure 3. Comparing Figure 2 and Figure 4, it is striking how similar the acoustic and electromagnetic data are. The main differ-

ence is the guided event. The response from the guided wave is marked in Figure 4. As will be demonstrated below, the transform from fictitious time to real frequency is such that it will weigh down late event relative to early events. The guided wave is an early event.

### From fictitious time to frequency

The data in Figure 4 is the starting point for the transformation to the diffusive frequency domain data. The transform kernel in equation 8 has a damping term, $e^{-\sqrt{\omega\omega_0}t'}$, and a phase term, $e^{i\sqrt{\omega\omega_0}t'}$. Figures 5 display the fictitious time domain electric field multiplied by the damping term for a frequency of 1 Hz. This dataset is a damped versions of the dataset in Figure 4. Let the damped field be denoted $\tilde{E}_i$, such that,

$$\tilde{E}_i(\mathbf{x},t'|\omega) = E'_i(\mathbf{x},t')e^{-\sqrt{\omega\omega_0}t'}. \quad (9)$$

The damping term is frequency dependent and the damping effect increases with increasing frequency.

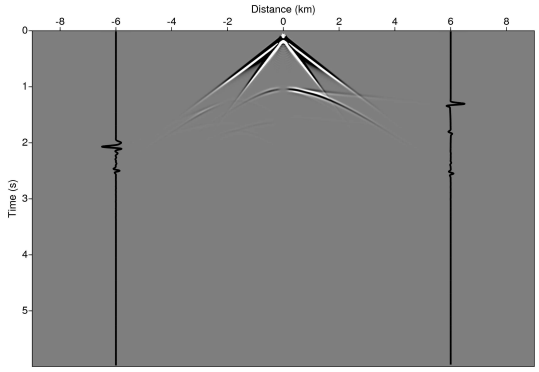


Figure 5: Damped normalized shotgather for the inline electric field. Frequency is 1.0 Hz. The traces at - 6 km offset and at +6 km offsets are shown strongly amplified.

From Figure 5 we observe that the damping effect is so strong that the guided event at approximately 1.25 s completely dominates at large positive offsets. The strong amplitude at large negative offsets is linked to the layer buried at 1 km below the seabed. For frequencies which are in the typical marine CSEM frequency band, we observe that at any offset the early arrivals give important contributions to the frequency domain data. Early arrivals at intermediate and large offsets are usually refracted and guided events. Reflections and diffractions at intermediate and large offsets are late arrivals. Their contribution is less important in marine CSEM compared to refracted and guided events. This effect is exposed by analyzing the marine CSEM experiment in the fictitious time domain where contributions from late arriving reflections are quenched by the transform function.

There is an additional effect in the transform from fictitious time to diffusive frequency that further reduce the relative contribution from reflections and diffractions. The effective transform frequency in equation 8 is relatively small favoring events that are slowly varying in time. Events like refractions and guided events will have waveforms that corresponds to the temporal integral of the waveforms for reflected and diffracted events, thus they are temporally smoothed events in the fictitious time domain. The contributions from these temporally smoothed refraction and guiding events are amplified compared to reflection and diffractions by the transform from fictitious time to frequency.

## CONCLUSIONS

The Maxwell equations in the quasi-static or diffusive limit can be transformed to a wave equation. The propagation of the fields can be analyzed in this transformed or fictitious time domain. Conclusions with regards to the real field propagation must take into account the properties of the inverse transform from the wave domain to the diffusive domain. There are two effects in the inverse transform that must be accounted for.

The first effect is that part of the inverse transform is an exponential damping of late arrivals. Thus, early arrivals in the wave domain are relatively more important than late arrivals. This effect becomes more pronounced with increased frequency. The recorded data in a marine CSEM survey configuration will be dominated by the first arrival if the frequency is sufficiently high. For a subsurface with a typical background resistivity of 1 ohm-m this happens for frequencies above approximately 1.0 Hz. First arrivals in the wave domain are refractions if the resistivity increases with depth. First arrivals can also be guided events if thin resistive layers are present in the subsurface.

The second effect is more subtle and is related to the phase term in the inverse transform in combination with waveform modifications for refracted and guided events. Refracted and guided events are smoothed compared to reflected and diffracted events. The smoothing effect amounts to an amplification of the low frequency part of the spectra. The result is that refracted and guided events make relatively large contributions to the inverse transform from fictitious time to frequency when compared with reflections and diffractions. Thus, if refractions and reflections are present with equal amplitude along the same time trace the inverse transform will give most weight to the refraction. This effect comes in addition to the damping of late arrivals which normally are reflections and diffractions. The smoothing effect is most important for frequencies up to 1.0 Hz. Above 1.0 Hz the inverse transform is dominated by the exponential damping term.

Concepts like reflections, refractions, diffractions and transmissions are valid for recorded events in a marine CSEM survey. Due to the the earth properties, the transmitter properties and the source/receiver configuration we conclude that marine CSEM data is dominated by refracted and potentially guided events. Typical for marine CSEM data are significant field amplitudes for low frequencies only, large source-receiver offsets and a high content of refraction events. These are attributes that are essential for the success of seismic full waveform inversion and may explain the relative success of full waveform inversion of marine CSEM data.

**EDITED REFERENCES**

Note: This reference list is a copyedited version of the reference list submitted by the author. Reference lists for the 2017 SEG Technical Program Expanded Abstracts have been copyedited so that references provided with the online metadata for each paper will achieve a high degree of linking to cited sources that appear on the Web.

**REFERENCES**

Carcione, J., 2007, Wave fields in real media: Wave propagation in anisotropic, anelastic, porous and electromagnetic media: Elsevier 38.

de Hoop, A. T., 1996, A general correspondence principle for time-domain electromagnetic wave and diffusion fields: Geophysical Journal International, **127**, 757–761, http://dx.doi.org/10.1111/j.1365-246X.1996.tb04054.x.

Lee, K. H., G. Liu, and H.F. Morrison, 1989, A new approach to modeling the electromagnetic response of conductive media: Geophysics, **54**, 1180–1192, http://dx.doi.org/10.1190/1.1442753.

Mittet, R., 2010, High-order finite-difference simulations of marine CSEM surveys using a correspondence principle for wave and diffusion fields: Geophysics, **75**, no. 1, F33–F50, http://dx.doi.org/10.1190/1.3278525.